Received: 16 April 2017 | Revised: 20 July 2017 | Accepted: 18 August 2017

DOI: 10.1002/ajpa.23304

RESEARCH ARTICLE

WILEY American Journal of PHYSICAL ANTHROPOLOGY

Cranial sexual dimorphism in the Kinda baboon (*Papio hamadryas kindae*)

Michelle Singleton[1] | Brielle C. Seitelman[2] | Joseph R. Krecioch[2] | Stephen R. Frost[3]

[1]Department of Anatomy, Chicago College of Osteopathic Medicine, Midwestern University, Downers Grove, Illinois

[2]Department of Anatomy, Midwestern University, Downers Grove, Illinois

[3]Department of Anthropology, University of Oregon, Eugene, Oregon

Correspondence
Michelle Singleton, Department of Anatomy, Chicago College of Osteopathic Medicine, Midwestern University, 555 31st Street, Downers Grove, IL 60515.
Email: msingl@midwestern.edu

Funding information
Wenner-Gren Foundation, Grant/Award Number: 6436; National Science Foundation, Grant/Award Number: BIR 902234; Research Foundation of the City University of New York, Grant/Award Number: 9-91980; Leakey Foundation

Abstract

Objectives: The smallest extant member of genus *Papio*, the Kinda baboon exhibits low sexual dimorphism and a distinctive cranial shape. Ontogenetic scaling accounts for most cranial-shape differences within *Papio*, but studies have shown that the Kinda follows a separate ontogenetic trajectory. If so, its cranial-dimorphism pattern should differ from other subspecies. To evaluate this hypothesis, morphometric analysis was used to investigate cranial dimorphism in *Papio*.

Materials and methods: Three-dimensional landmarks were digitized on 434 adult crania representing six *Papio* subspecies. Size- and shape-dimorphism magnitudes were quantified using centroid size and Procrustes distances. Patterns of sex- and size-related variation were explored using MAN(C)OVA, multivariate regression, and form-space PCA. Canine dimorphism was investigated using dental metrics.

Results: Kinda size and shape dimorphism are significantly lower than in other *Papio* subspecies. The relative magnitude of Kinda shape dimorphism is similar to other southern baboons; Kinda canine dimorphism is unremarkable. MAN(C)OVA results support subspecies differences in cranial dimorphism and scaling. Allometric and dimorphism vectors differ significantly in some subspecies, and their vector-angle matrices are strongly correlated. The Kinda's allometric vector angles are divergent. Form-space PC3, summarizing size-independent dimorphism, separates the Kinda from other subspecies.

Discussion: The Kinda baboon exhibits significantly lower size and shape dimorphism than other baboons, but its relative dimorphism levels are unexceptional. The Kinda differs from other subspecies in patterns of allometry, size-related shape dimorphism, and residual shape dimorphism. Kinda facial shape is "masculinized" relative to size, especially in females, suggesting female sexual selection contributed to the evolution of Kinda dimorphism.

KEYWORDS
allometry, allotaxa, geometric morphometrics, hybridization, social structure

1 | INTRODUCTION

The Kinda baboon (*Papio hamadryas kindae*) is the smallest extant member of genus *Papio* (Delson et al., 2000). Once considered a small variant of the yellow baboon (*P. h. cynocephalus*), the Kinda is now recognized as a separate subspecies (Burrell, Jolly, Tosi, & Disotell, 2009; Freedman, 1963; Groves, 2001; Grubb et al., 2003; Weyher, Phillips-Conroy, Fourrier, & Jolly, 2014; Zinner, Groeneveld, Keller, & Roos, 2009; Zinner, Wertheimer, Liedigk, Groeneveld, & Roos, 2013). In addition to its characteristic pelage and low body mass, the Kinda exhibits reduced sexual size dimorphism and a distinctive cranial morphology (Freedman, 1963; Jolly, Burrell, Phillips-Conroy, Bergey, & Rogers, 2011; Leigh, 2006; Weyher et al., 2014). Because ontogenetic scaling accounts for the majority of cranial-shape variance within and among subspecies of *Papio* (Dunn, Cardini, & Elton, 2013; Freedman, 1962; Frost, 2013; Frost, Marcus, Reddy, Bookstein, & Delson, 2003; Leigh,

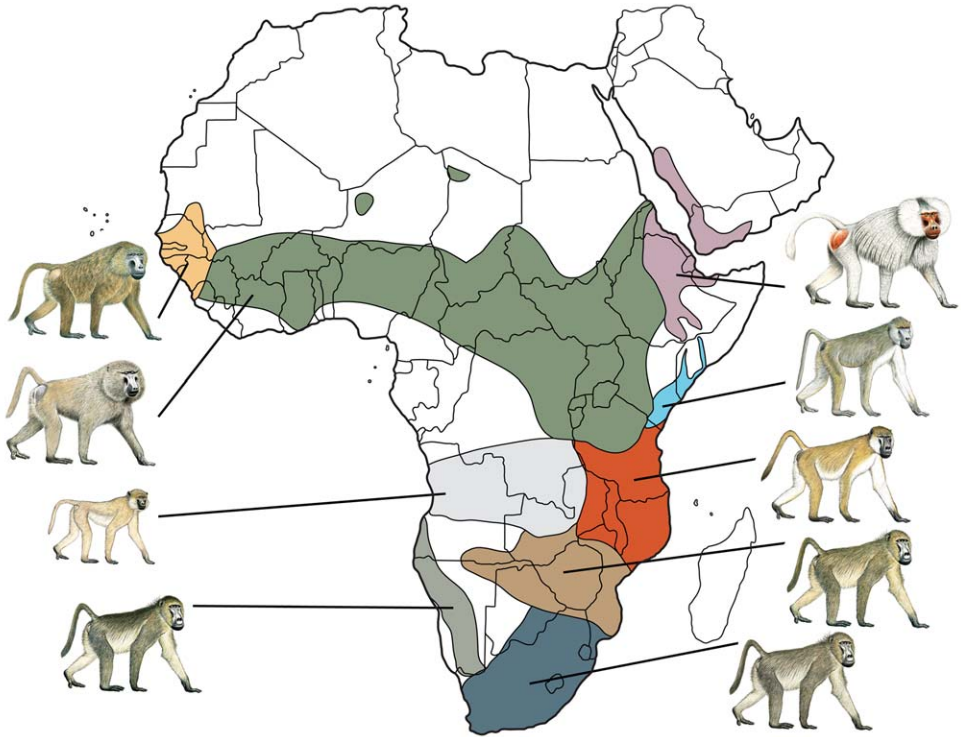

FIGURE 1 External morphology and geographical distribution of recognized baboon allotaxa. Clockwise from upper right: hamadryas baboon, yellow baboon (*ibeanus* and *cynocephalus* variants), chacma baboon (*griseipes*, *ursinus*, and *ruacana* variants), Kinda baboon, olive baboon, and Guinea baboon. Distribution map adapted with permission from Kenneth Chiou (Chiou, 2013) under Creative Commons Attribution 3.0 Unported License. Baboon illustrations © 2013 Stephen D. Nash/IUCN SSC Primate Specialist Group. Used with permission

2006), the Kinda cranium has sometimes been characterized as pedomorphic (Dunn et al., 2013; Frost et al., 2003; Jolly, 2003). However, many Kinda cranial traits are size-independent, and it diverges from the shared baboon ontogenetic trajectory (Leigh, 2006). One might, therefore, expect the Kinda's pattern of cranial dimorphism to differ from other subspecies. To address this question, this study examines sexual dimorphism in *Papio* and tests the hypothesis that *Papio hamadryas kindae* differs from other baboons in its pattern of cranial sexual dimorphism.

2 | BACKGROUND

Papio (Cercopithecinae: Papionini) is a highly successful pan-African radiation of large-bodied, terrestrial monkeys (Groves, 2001; Jolly, 1993; Kingdon, 1997). It comprises at least six phenotypically distinct allotaxa[1] (Figure 1), which differ in body size, cranial morphology, pelage characteristics, tail carriage, social-group structure, and mating system (Frost et al., 2003; Groves, 2001; Grubb, 1999; Jolly, 1993, 2003; Kingdon, 1997; Leigh, 2006). Molecular phylogenetic and morphological analyses support a deep evolutionary divergence (~2 Mya) between hamadryas, olive, and Guinea baboons in the north, versus chacma, yellow, and Kinda baboons in the south (Burrell, 2009; Frost, 2013; Frost et al., 2003; Zinner et al., 2009; Zinner et al., 2013).

2.1 | *Papio hamadryas kindae*

The smallest extant member of genus *Papio* (Delson et al., 2000), the Kinda baboon occupies a range (Figure 1) across southwest Tanzania, parts of the Democratic Republic of Congo and Zambia, and northern Angola (Zinner, 2013). Long considered a small variant of the yellow baboon, *Papio h. cynocephalus*, the Kinda is now recognized as an independent, relatively ancient offshoot (mtDNA divergence ~1.5 Mya) of a southern African mitochondrial lineage that also includes the gray-footed chacma (*P. h. ursinus griseipes*) and central African yellow baboon populations (Burrell, 2009; Grubb et al., 2003; Jolly et al., 2011; Liedigk, Roos, Brameier, & Zinner, 2014; Zinner et al., 2009; Zinner et al., 2013).

Phenotypically, the Kinda is easily distinguished from the yellow baboon (Figure 2) by its paler, silkier adult coat; darker contrasting "mohawk"; white (versus black) infant coat; pink circumorbital skin resembling spectacles; and curved (versus broken) tail carriage (Groves, 2001; Jolly et al., 2011; Weyher et al., 2014; Zinner, 2013). The Kinda is further distinguished from other baboons by its reduced sexual size

[1]Extant *Papio* allomorphs interbreed freely in areas of sympatry, and molecular studies have found widespread mitochondrial paraphyly within and between the northern and southern baboon clades, suggesting a long history of introgressive hybridization (Burrell, 2009; Jolly, 1993, 2003; Jolly et al., 2011; Newman, Jolly, & Rogers, 2004; Phillips-Conroy, & Jolly, 1986; Phillips-Conroy, Jolly, & Brett, 1991; Samuels & Altmann, 1986; Wall et al., 2016; Wildman et al., 2004; Zinner, 2013; Zinner et al., 2009). In recognition of their extensive hybridization and clinal pattern of cranial variation, we follow Frost et al. (2003) in referring to *Papio* allotaxa as biological subspecies of *P. hamadryas* rather than full-rank phylogenetic species.

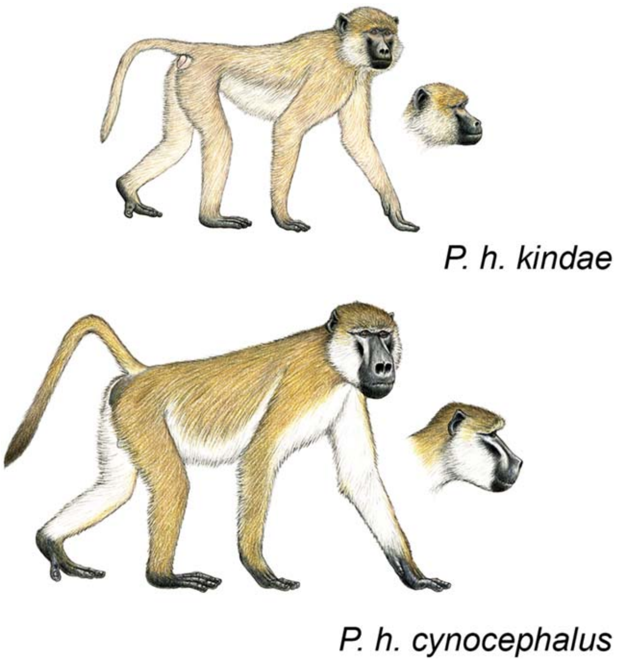

FIGURE 2 The Kinda baboon (top) is distinguished from the yellow baboon (bottom) by its small size, gracile build, pale coat, pink circumorbital skin, curved (versus broken) tail carriage, and moderate facial prognathism (Groves, 2001; Jolly et al., 2011; Leigh, 2006; Weyher et al., 2014; Zinner, 2013). Baboon illustrations © 2013 Stephen D. Nash / IUCN SSC Primate Specialist Group. Used with permission

dimorphism, gracile body build, and cranial morphology characterized by a sharply angled midfacial profile; moderate facial prognathism; a narrow anterior rostrum; broad zygomatics; and a relatively globular neurocranium (Freedman, 1963; Frost et al., 2003; Groves, 2001; Jolly, 1993; Jolly et al., 2011; Leigh, 2006; Weyher et al., 2014; Zinner, 2013).

Like olive, chacma, and yellow baboons, the Kinda has a multimale, multifemale social structure with female philopatry and male dispersal (Burrell, Jolly, Rogers, Phillips-Conroy, & Disotell, 2011; Jolly et al., 2011; Weyher et al., 2014). However, Kinda baboons exhibit several unique behavioral characteristics. Kinda females give alarm calls similar to those of male baboons; male calls are higher pitched than in other taxa; and copulatory calls have not been observed in either sex (Chiou, 2013; Phillips-Conroy, Jolly, Burrell, Rogers, & Weyher, 2009a; Phillips-Conroy, Jolly, & Weyher, 2009b). Additionally, Kinda males exhibit a unique pattern of affiliative behavior in which males initiate over 90% of male–female dyadic encounters and perform the majority of grooming (Figure 3), while females are responsible for termination of most interactions (Phillips-Conroy et al., 2009a, 2009b; Weyher et al., 2014). Male grooming frequency and duration are largely independent of female reproductive status or the presence of infants (Weyher et al., 2014). For this reason, it has been proposed that Kinda males pursue an alternative mating strategy based on "male investment in mates and/or their infants" versus competition to maximize short-term mating opportunities (Weyher et al., 2014). This hypothesis is broadly consistent with Leigh's (2006) conjecture that relaxed sexual selection has limited both evolutionary size increase and sexual shape dimorphism in the Kinda lineage.

2.2 | Cranial variation in *Papio*

Allometric scaling accounts for a high proportion of cranial-shape variation within *Papio* (Frost et al., 2003; Leigh, 2006). Within subspecies, males and females follow common ontogenetic trajectories, and sexual dimorphism is primarily the result of differences between males and females in the rate and/or duration of cranial growth (Freedman, 1962; Leigh, 2006; Leigh & Cheverud, 1991). Similarly, *Papio* subspecies follow similar ontogenetic trajectories, and allometric scaling contributes substantially to intersubspecies differences in neurocranial proportions and facial prognathism (Freedman, 1962; Frost et al., 2003; Leigh, 2006). Because of its small size, the Kinda baboon has sometimes been characterized as pedomorphic relative to other subspecies (Frost et al., 2003; Jolly, 2003). However, Leigh (2006) found that the Kinda departs from the common baboon ontogenetic trajectory, leading him to suggest that Kinda development is characterized by an acceleration of cranial shape change relative to size. If the Kinda's ontogenetic scaling patterns are indeed different from other baboons, one might reasonably expect it to differ in its pattern of cranial sexual dimorphism.

Because sexual dimorphism in *Papio* is inextricably linked to size and scaling relationships (Freedman, 1962; Frost et al., 2003; Leigh & Cheverud, 1991), these factors must be fully integrated into any analysis of variation related to dimorphism. To test the hypothesis that *Papio hamadryas kindae* differs from other baboons in its pattern of cranial sexual dimorphism, this study examines variation in absolute cranial size, cranial scaling patterns, magnitude of absolute and relative shape dimorphism, and patterns of size-related and size-independent shape dimorphism. Because it is an important aspect of sexual dimorphism in catarrhines and is independent of allometric cranial dimorphism in

FIGURE 3 Typical Kinda baboon grooming dyad. Males initiate over 90% of male–female dyadic encounters and perform the majority of grooming; female Kindas are responsible for termination of most interactions (Phillips-Conroy et al., 2009a,b; Weyher et al., 2014). Photo courtesy of Anna Weyher, Kasanka Baboon Project. Used with permission

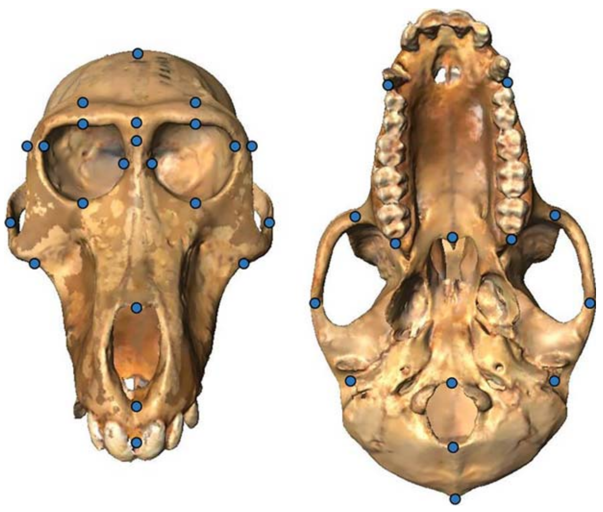

FIGURE 4 Three-dimensional craniometric landmarks used in this study. Landmark descriptions are provided in Appendix 1 (Frost et al., 2003). Female *Papio h. anubis* cranium courtesy of the Smithsonian Institution–National Museum of Natural History

Papio (Fleagle, 2013; Frost et al., 2003), canine dimorphism is also examined using standard dental metrics.

3 | MATERIALS AND METHODS

3.1 | Craniometric data

The cranial data set for this study comprised 34 3D craniofacial landmarks (Figure 4 and Appendix 1) collected on 434 adult crania representing six *Papio* subspecies (Table 1). Unequal representation of sexes and subspecies in this sample reflects historical geographical biases in museum holdings and early collectors' apparent preference for male specimens. All data were collected by S.F. using a Microscribe 3D-X® digitizer following the protocol described in Frost et al. (2003). Dorsal and ventral aspects of each cranium were digitized separately and subsequently aligned using a least-squares fitting procedure (Frost et al., 2003). Generalized Procrustes analysis was used to align specimens in a common shape space and eliminate the nuisance parameters of location, rotation, and scale (Bookstein, 1996; Dryden & Mardia, 1998; Gower, 1966). Each specimen was averaged with its superimposed reflection to symmetrize landmark configurations and estimate missing bilateral landmarks (Mitteroecker & Gunz, 2009). Landmark data are available upon request via the NYCEP PRIMO data repository (NYCEP, 2013). Standard dental measurements collected on a separate series of *Papio* crania (Table 1) by J. Michael Plavcan (1990) are used here with his permission. The Plavcan (1990) data, collected using a reticle, were supplemented by caliper measurements taken by M.S. on olive and chacma specimens housed in the University of California–Museum of Vertebrate Zoology. With the exception of a single *P. h. hamadryas* female with heavier wear, all Plavcan specimens possessed fully erupted, unbroken canines scored as having either "light" or "moderate" wear judged unlikely to impact dental dimensions (Plavcan & Van Schaik, 1992). Similarly, all UCMVZ specimens possessed fully erupted canines with light or moderate wear and intact tips. Bivariate plots and *t*-tests showed no meaningful differences between caliper and reticle measurements for either subspecies. Separate analyses conducted with the combined data and the Plavcan sample alone yielded virtually identical results, so results are presented only for the larger combined sample (Table 1).

3.2 | Cranial dimorphism magnitude

For each subspecies, cranial size was quantified using centroid size (CS), the standard measure of scale in GM analyses (Dryden & Mardia, 1998; Slice, Bookstein, Marcus, & Rohlf, 1996). Dimorphism was calculated both as the easily interpretable ratio of male and female mean centroid sizes CS_M/CS_F and as the log-ratio $\ln(CS_M/CS_F)$, which is equivalent to the male–female log-size difference $\Delta \ln CS$ (Smith, 1981). The magnitude of cranial shape dimorphism was quantified as the Procrustes distance *d* between male and female mean landmark configurations. Procrustes distance is equivalent to the Euclidean distance in shape space between two optimally superimposed landmark sets and summarizes overall shape disparity (Bookstein, 1991; Slice et al., 1996). An index of relative shape dimorphism $d/\Delta \ln CS$ was calculated to represent the magnitude of shape difference relative to size difference, and covariation in size and shape dimorphism were examined by correlation analysis.

TABLE 1 Comparative samples by subspecies and sex

	Taxon	Cranial sample		Dental sample	
		Female	Male	Female	Male
Northern					
Olive	*P. h. anubis*	48	103	10 (3/7)	15 (6/9)
Hamadryas	*P. h. hamadryas*	4	25	5	21
Guinea	*P. h. papio*	1	16	0	0
Southern					
Yellow	*P. h. cynocephalus*	8	19	6	9
Chacma	*P. h. ursinus*	75	106	4 (3/1)	10 (4/6)
Kinda	*P. h. kindae*	14	15	14	9

Cranial data drawn from Frost et al. (2003) are archived in the NYCEP PRIMO database (NYCEP, 2013). Dental measurements drawn from Plavcan (1990) were supplemented with caliper measurements taken by M.S. on chacma and olive baboon dentitions (University of California–Museum of Vertebrate Zoology), with subsamples indicated as follows: Total *N* (reticle/caliper).

TABLE 2 Cranial size and shape dimorphism in *Papio*

Subspecies	CS_M/CS_F	ΔlnCS	*d*	*d*/ΔlnCS	MLD	CHTD
P. h. ursinus	1.24	0.2150	0.0913	0.4244	1.07	3.67
P. h. cynocephalus	1.23	0.2098	0.0841	0.4008	1.10	2.85
P. h. anubis	1.23	0.2042	0.0786	0.3847	1.03	2.39
P. h. hamadryas	1.22	0.1995	0.0915	0.4588	1.05	2.74
P. h. papio	1.19	0.1724	0.0801	0.4648	—	—
P. h. kindae	**1.15**	**0.1423**	**0.0624**	0.4387	1.07	2.80
P value (Kinda vs *Papio*)	<0.0001	<0.0001	<0.0001	0.7774	0.7289	0.3526

Abbreviations: CS = mean centroid size; *d* = Procrustes distance between male and female means; ΔlnCS = $\ln(CS_M/CS_F)$; MLD = molar length dimorphism; CHTD = canine height dimorphism; *P* value = one-tailed probability (*Z* test).

3.3 | Cranial dimorphism patterning

Differences in shape dimorphism patterns were tested using multivariate analysis of variance (MANOVA) and angular comparisons of multivariate regression vectors (Drake & Klingenberg, 2008; Frost et al., 2003; Slice, 2005). Following Frost et al. (2003), principal components analysis (PCA) was applied as a data reduction method, and scores for PCs 1–10, summarizing 84.5% of total shape variance, were used for subsequent parametric analyses. Two-way MANOVA of the PC scores by subspecies and sex was used to test for differences in sexual dimorphism patterns among subspecies. A statistically significant subspecies-by-sex interaction term would reject the hypothesis that dimorphism patterns are shared across subspecies of *Papio* (Frost et al., 2003).

Shape dimorphism vectors were estimated for each subspecies by multivariate regression of the Procrustes coordinate matrix on sex (Drake & Klingenberg, 2008; Slice, 2005). Dimorphism vectors were also calculated for the entire sample using both Procrustes coordinates and residuals from the regression of Procrustes coordinates on the natural logarithm of centroid size (lnCS) (Klingenberg, 2016). The two sets of vectors summarize patterns of total sexual dimorphism and size-independent (residual) dimorphism, respectively. Associated patterns of cranial shape variation were visualized in *Morpheus et al*. (Slice, 1998).

The angular difference between subspecies' dimorphism vectors was calculated as the arccosine of their vector correlation (dot product) (Zelditch, Swiderski, Sheets, & Fink, 2004). Small angles indicate similar vector orientations and dimorphism patterns, while large angles indicate divergent vectors and disparate dimorphism patterns. Following McNulty, Frost, and Strait (2006), statistical significance of vector angles was tested using a random permutation test ($N = 10{,}000$). Up to 20 males and 20 females were drawn at random from each subspecies and randomly reassigned to subspecies, the angle was calculated between permuted group vectors, and the original angle then compared to the distribution of permuted values to determine its probability under the null hypothesis that all specimens are drawn from a single population. Observed angles were considered statistically significant at a Šidák-adjusted $\alpha = 0.0034$ (Good, 2000; Šidák, 1967; Zelditch et al., 2004).

To explore the relationship between allometry and sexual dimorphism, allometric shape vectors were estimated using form-space PCA (FPCA) and multivariate regression of Procrustes coordinates on lnCS (Drake & Klingenberg, 2008; Klingenberg, 1996; Mitteroecker, Gunz, Bernhard, Schaefer, & Bookstein, 2004). Similarity of subspecies' scaling patterns was tested using angular comparisons of subspecies FPC1 and size-regression vectors using the permutation procedure described above. Correlations between vectors summarizing allometric variation and dimorphism were calculated for each subspecies. The correlation between matrices of regression and dimorphism vector angles was used to estimate the contribution of allometry to sexual shape dimorphism. Full-sample regression and FPCA analyses, as well as an FPCA of subspecies male and female mean shapes, were used to explore size-correlated and residual dimorphism trends. Associated patterns of cranial shape variation were compared using wireframe visualizations. Generalized Procrustes analysis and visualizations were executed in *Morpheus et al*. (Slice, 1998), and statistical analyses were performed in *SAS* 9.3®.

3.4 | Canine dimorphism

Canine crown height (CHT) is the most variable measurement of canine size in both males and females and is also the most directly relevant to the canine's use as a weapon and in agonistic display (Greenfield & Washburn, 1991; Plavcan, 1993). Dimorphism in maxillary canine crown height (CHTD) and first molar mesiodistal crown length (M1LD) were calculated as the ratio of male and female mean values, CHT_M/CHT_F and $M1L_M/M1L_F$, and their natural log transformations (Smith, 1981). Additionally, relative canine height was calculated for males and females of each subspecies following the method of Plavcan, Van Schaik, and Kappeler (1995). Residuals were calculated from an isometric least-squares regression line fitted through a combined sex plot of lnCHT against lnM1L. A plot of average female versus male residual canine height (rCHT) was used to evaluate subspecific differences in relative female canine height.

4 | RESULTS

4.1 | Magnitude of cranial dimorphism

Measures of cranial dimorphism are lower in *P. h. kindae* than in other baboon subspecies (Table 2). The cranial size dimorphism ratio

CS_M/CS_F is 1.15 in the Kinda versus an average of 1.22 for other subspecies, and this difference is statistically significant (one-tailed *t*-test, $P < .0001$). Likewise, the average male-female Procrustes distance is 0.0624 versus an average of 0.0851 for other subspecies (one-tailed $P < .001$). However, the Kinda's index of relative size dimorphism (d/ΔlnCS) is similar to *P. h. ursinus* and not significantly different from other subspecies ($P = 0.78$).

4.2 | Magnitude of canine dimorphism

Consistent with prior studies, molar size dimorphism in *Papio* is low, while canine height dimorphism varies across the five baboon subspecies for which both male and female values were available (Table 2). Hamadryas, yellow, and Kinda baboons showed similar dimorphism values, while the olive and chacma baboons showed comparatively low and high dimorphism values, respectively. A bivariate plot of female versus male lnCHT (Figure 5a) shows a roughly isometric relationship between male and female mean CHT in the three former subspecies. Olive females have taller canines relative to males, while chacma females have comparatively short canines (Figure 5a). A plot of female versus male rCHT (Figure 5b) shows a similar pattern. Kinda, hamadryas, and yellow baboons fall close to the reduced major axis line (Plavcan, 1990), while the olive and chacma baboons fall well above and below the line, respectively.

4.3 | Subspecies dimorphism patterns

The MANOVA of overall sexual dimorphism returns statistically significant subspecies, sex, and interaction effects ($P < .0001$), indicating that differences in shape dimorphism patterns among subspecies are present. However, direct pairwise comparisons of subspecies dimorphism regression vectors are mostly nonsignificant (Table 3). Relatively large vector angles for Guinea and hamadryas baboons could either reflect actual pattern differences or the effect of small sample sizes. The Kinda baboon's vector orientation is most similar to those of its fellow southern subspecies, the chacma and yellow baboons, forming angles of 22.5° and 23.4°, respectively. Shape differences between the average male and female Kinda are generally consistent with patterns of shape variation summarized by the common *Papio* dimorphism vector (Figure 6). In comparison with yellow and chacma baboons (Figure 6), the Kinda exhibits a similar pattern but lesser degree of dimorphism in facial prognathism, klinorhynchy, and neurocranial shape. Zygomatic breadth dimorphism is notably absent in the Kinda.

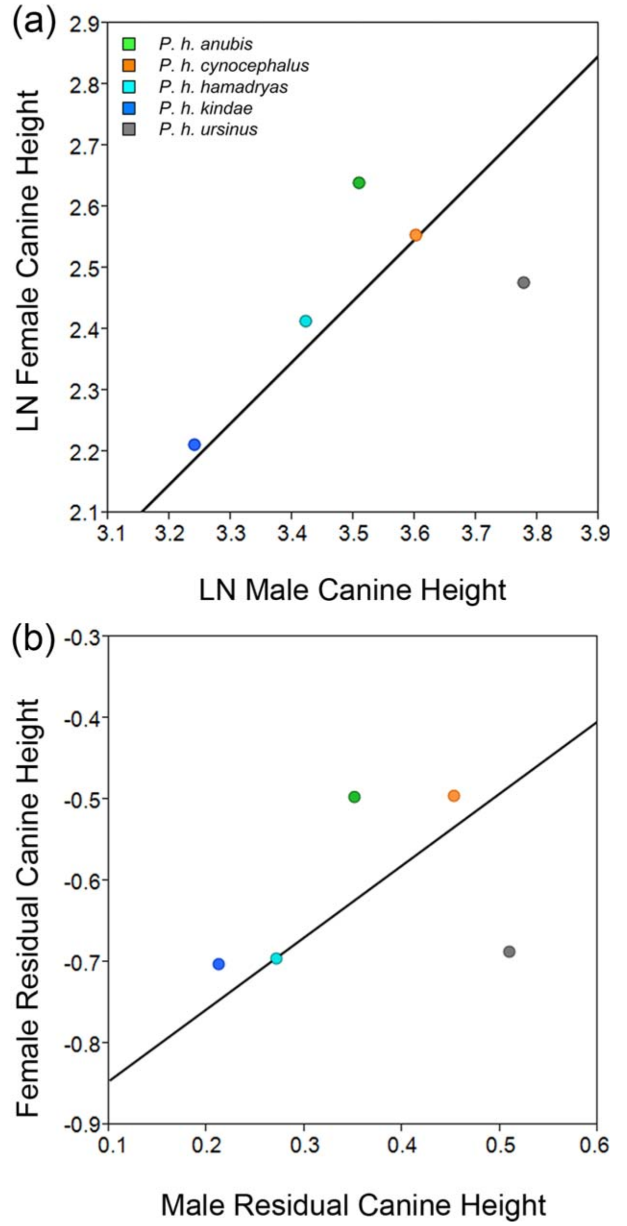

FIGURE 5 Canine dimorphism in *Papio*. (a) Isometric line fitted to a plot of female versus male canine height (mean lnCHT). (b) Reduced major axis line fitted to a plot of female versus male residual canine height (mean rCHT). Canine dimorphism patterns in the Kinda, hamadryas, and yellow baboons are similar. Relatively large female canines in the olive baboon are associated with reduced canine dimorphism. Relatively large male canines in the chacma baboon contribute to its higher dimorphism level

4.4 | Subspecies scaling patterns

MANCOVA of size-correlated shape variation returns statistically significant subspecies, size, and interaction effects ($P < .0001$), supporting the presence of subspecies differences in allometric scaling (Frost et al., 2003). Direct pairwise comparisons of subspecies size-regression vectors are mostly nonsignificant (Table 4). The Kinda's vector orientation is significantly different from the Guinea and hamadryas baboons (Šidák-adjusted $\alpha = 0.0034$); however, the large vector angles for the latter subspecies suggest caution should be exercised with respect to these findings. The Kinda baboon's regression-vector orientation is most similar to the chacma and yellow baboons, forming angles of 22.6° and 25.1°, respectively. However, the latter subspecies have smaller angles with the olive baboon and each other than either does with the Kinda. Comparisons of subspecies FPC1 vectors yielded both smaller angles and lower *P* values for most subspecies pairs (Table 4). The Kinda is

TABLE 3 Angular comparison of sexual dimorphism vectors

Angle\P	Pha	Phc	Phh	Phk	Php	Phu
P. h. anubis	–	0.3117	0.8644	0.3017	0.1228	0.6333
P. h. cynocephalus	22.3	–	0.3109	0.1956	0.6305	0.2167
P. h. hamadryas	19.6	31.0	–	**0.0023**	0.0553	0.4168
P. h. kindae	27.1	23.4	31.7	–	**0.0024**	0.4314
P. h. papio	41.9	32.8	49.4	39.9	–	0.2299
P. h. ursinus	14.8	21.7	24.4	22.5	36.2	–

Below diagonal: sexual-dimorphism vector angles (°); above diagonal: *P* value (10,000 permutations).
Bold = significant at Šidák-adjusted $\alpha = 0.0034$.

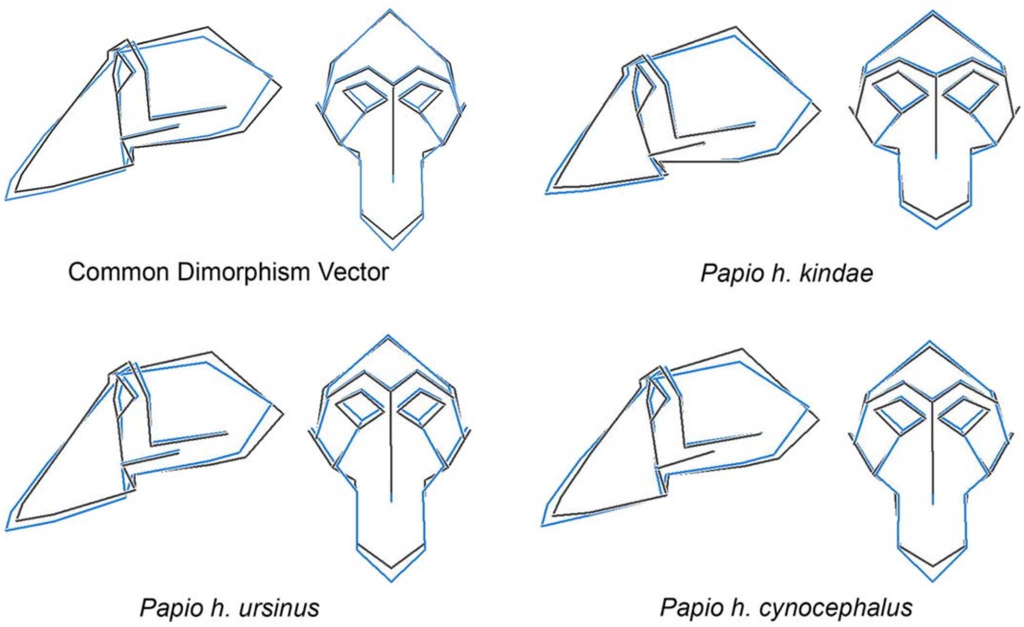

FIGURE 6 Sexual shape dimorphism in *Papio*. Wireframes represent average female (black) and male (blue) cranial shapes. Shape dimorphism in the Kinda baboon (top right) is consistent with patterns of shape variation summarized by the common *Papio* dimorphism vector (top left). In comparison with chacma and yellow baboons (bottom left, right), the Kinda exhibits less dimorphism in facial prognathism, klinorhynchy, and neurocranial shape; zygomatic breadth dimorphism is absent in the Kinda

TABLE 4 Angular comparison of allometric vectors

	Pha	Phc	Phh	Phk	Php	Phu
P. h. anubis	–	7.3	7.5	**10.3**	27.8*	6.8
P. h. cynocephalus	20.1	–	11.3	9.5*	25.6	7.4
P. h. hamadryas	19.5	30.4	–	**12.5**	27.9*	9.3
P. h. kindae	27.6	25.1	**33.1**	–	28.4	**8.8**
P. h. papio	47.7	41.0	50.6*	**49.1**	–	24.3*
P. h. ursinus	16.8	19.1	24.6	22.6	39.9	–

Below diagonal: size-regression vector angles (°); above diagonal: form-space PC1 vector angles (°).
Bold = significant at Šidák-adjusted $\alpha = 0.0034$; *significant at unadjusted $\alpha = 0.05$.

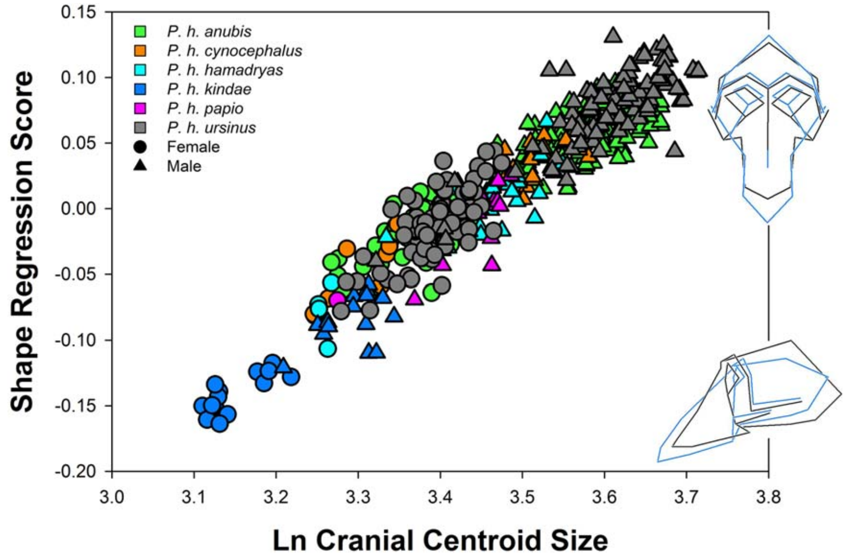

FIGURE 7 Shared cranial scaling pattern in *Papio*. Plot of multivariate regression scores (Drake & Klingenberg, 2008) on cranial centroid size (lnCS). Wireframes represent extremes of size-correlated shape variation associated with small (black) and large (blue) cranial size

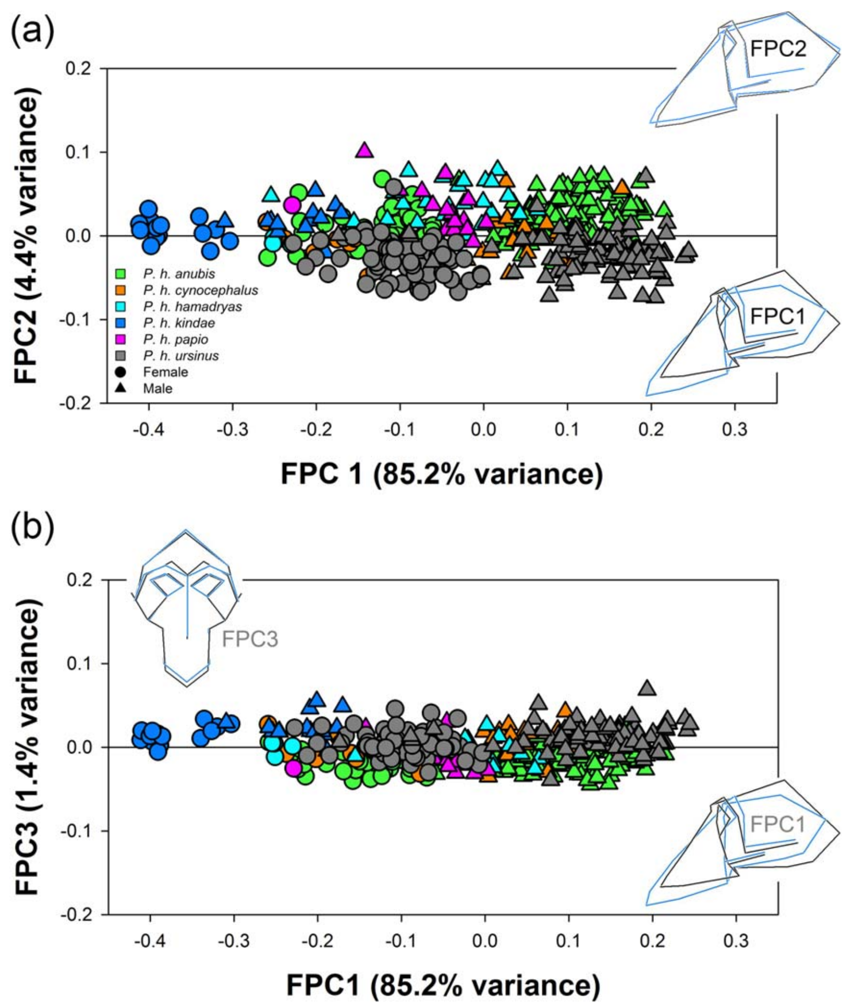

FIGURE 8 Full-sample form-space PCA. Wireframes represent negative (black) and positive (blue) extremes of form variation associated with each FPC. (a) FPC1 summarizes allometric shape variation including size-correlated dimorphism; FPC2 summarizes size-independent shape differences between northern and southern subspecies; (b) FPC3 summarizes size-independent sexual shape dimorphism

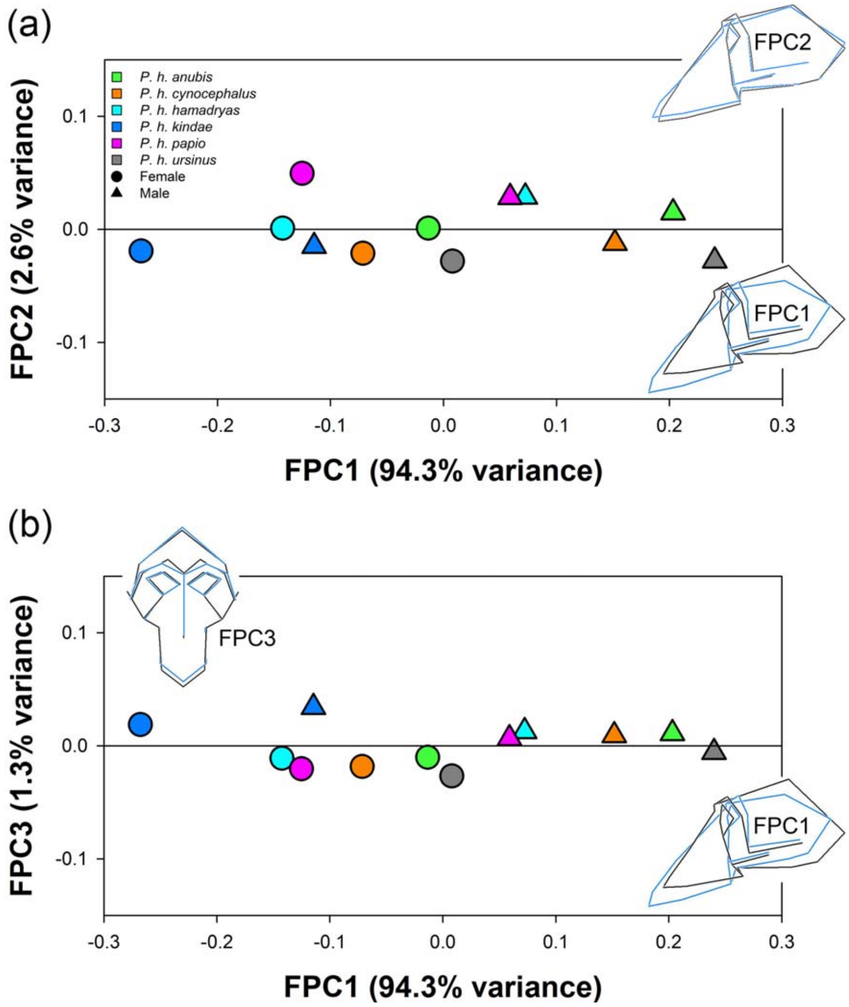

FIGURE 9 Form-space PCA of subspecies male and female means. Wireframes represent negative (black) and positive (blue) extremes of form variation associated with each FPC. (a) FPC1 and FPC2 summarize allometric and taxonomic shape variation, respectively. (b) FPC3 separates male and female means within subspecies. Both male and female Kinda exhibit relatively positive FPC3 scores

significantly different from chacma, hamadryas, and olive baboons at Šidák-adjusted $\alpha = 0.0034$ and from the yellow baboon at unadjusted $\alpha = 0.05$. Yellow and chacma vectors are again more similar to that of the olive baboon than either is to the Kinda.

4.5 | Allometric shape variation

Consistent with many prior studies, *Papio* allometric vectors—both size-regression and FPC1—separate subspecies and sexes and summarize variation in neurocranial proportions, facial proportions, and facial kyphosis (Frost et al., 2003; Leigh, 2006; O'Higgins & Collard, 2002; Singleton, 2002). Greater size (equivalent to more positive FPC1 scores) is associated with a relatively smaller, flatter neurocranium; longer and more ventrally oriented rostrum; and decreased midfacial (zygomatic) breadth (Figures 7 and 8). In matrix correlation tests (Bowley, 2014; Piepho, 2005), angular differences among subspecies shape-dimorphism vectors are strongly correlated with angular differences among allometric vectors (Mantel: FPC1, $r = 0.91$, $P = .001$; Size Reg. $r = 0.97$, $P = .002$), supporting a close relationship between size and shape dimorphism patterns.

4.6 | Residual (size-independent) shape variation

FPC2 scores are not significantly correlated with size ($r = 0.03$, $P = .47$) and exhibit a south-to-north gradient from chacma baboons (negative) through hamadryas baboons (positive). Analysis of variance of FPC2 scores finds a significant difference between the southern and northern baboon clades ($F = 232.91$, $P < .0001$). This finding replicates previous studies of baboon cranial variation whose results were based on size-corrected data (Dunn et al., 2013; Frost et al., 2003). Also consistent with these studies, as well as Leigh (2006), the lower FPC2 scores of southern subspecies reflect increased klinorhynchy and a relatively taller, narrower midface compared to northern baboon subspecies of similar size (Figures 8a and 9a).

FPC3 scores (Figures 8b and 9b) are also not significantly correlated with size ($r = 0.03$, $P = .56$) and separate males (more positive scores) from females (more negative scores). For the full-sample analysis (Figure 8b), average male FPC3 scores exceed average female scores in all subspecies except *P. h. hamadryas* (Table 5 and Figure 10). These differences are statistically significant at $P < .05$ in olive, Kinda, and chacma baboons; however, the remaining subspecies, which have

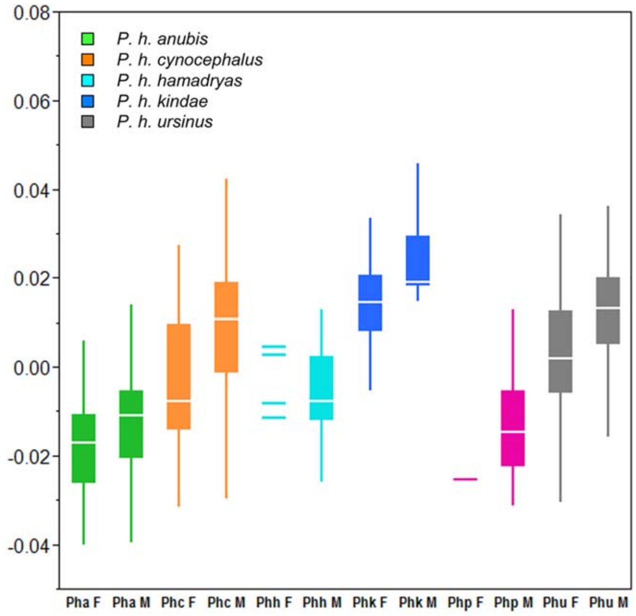

FIGURE 10 Distribution of full-sample FPC3 scores by subspecies and sex. White horizontal lines represent median values. Colored horizontal lines represent individuals. Boxes and whiskers represent quartiles and ranges, respectively. In the full-sample analysis, median and mean male FPC3 scores exceed female scores in all subspecies except *P. h. hamadryas* (Table 5)

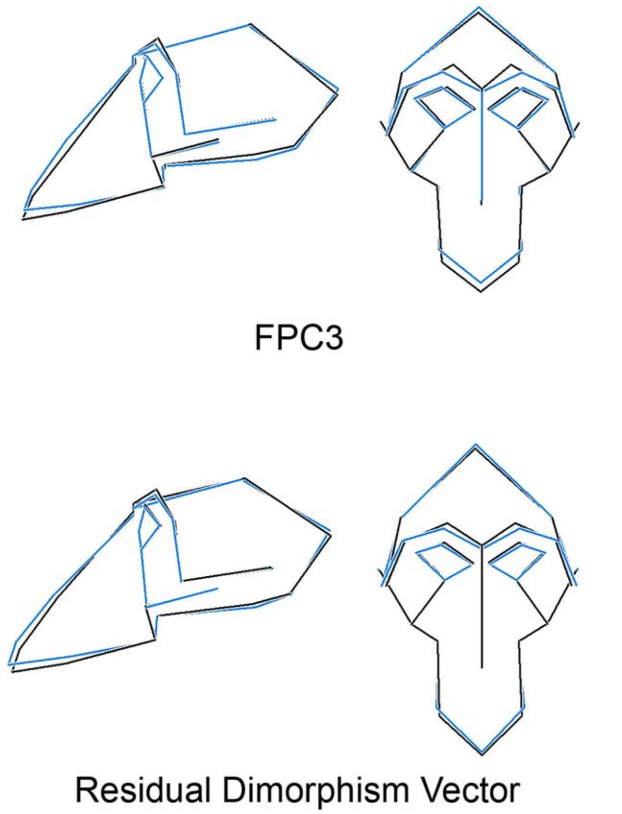

FIGURE 11 Size-independent sexual dimorphism in *Papio*. Wireframes represent extremes of shape variation summarized by FPC3 (top) and the sexual dimorphism vector computed on size-adjusted Procrustes coordinates (bottom). In each case, variation at the male end of the spectrum (blue) is characterized by increased relative facial breadth

small, unbalanced samples, do not achieve significance. Despite some overlap between subspecies and sexes, male scores are also significantly higher than female scores for *Papio* as a whole ($P = .03$). In the FPCA of male and female means (Figure 9b), which is less affected by small and/or unbalanced samples, male scores exceed female scores in all *Papio* subspecies. Taken together, these results suggest this axis summarizes residual shape dimorphism.

On FPC3, males exhibit greater zygomatic breadth and a broader anterior palate relative to consubspecific females (Figures 8b and 9b). This pattern of shape variation is consistent with many prior studies that have identified differences in relative facial breadth and palate proportions between catarrhine males and females (Frost et al., 2003; Leigh, 2006; Singleton, 2002; Weston, Friday, Johnstone, & Schrenk, 2004). Interpretation of FPC3 as an axis of size-independent sexual dimorphism is also supported by the regression of size-corrected coordinates on sex. This analysis, which directly examines residual sexual dimorphism, yields a pattern of variation in facial breadth and anterior palate dimensions extremely similar to FPC3 (Figure 11).

Interestingly, FPC3 also separates the Kinda baboon, with more positive mean scores, from all other subspecies (Figures 8b, 9b, and 10), and this difference is statistically significant (ANOVA $F = 53.96$, $P < .0001$; *post hoc* Tukey-adjusted $P < .001$). Notably, more "male-like" scores are seen for female, as well as male, Kinda (Figures 9b and 10).

TABLE 5 Mean FPC3 scores by subspecies and sex

		Full-sample FPC3			Mean FPC3		
Taxon	Abbr.	Female	Male	Diff.	Female	Male	Diff.
P. h. anubis	Pha	−0.0171	−0.0121	0.0050	−0.0102	0.0109	0.0211
P. h. cynocephalus	Phc	−0.0041	0.0077	0.0118	−0.0183	0.0092	0.0276
P. h. hamadryas	Phh	−0.0001	−0.0039	−0.0038	−0.0110	0.0127	0.0237
P. h. kindae	Phk	0.0150	0.0249	0.0099	0.0187	0.0341	0.0154
P. h. papio	Php	−0.0173	−0.0100	0.0073	−0.0204	0.0066	0.0269
P. h. ursinus	Phu	0.0037	0.0130	0.0093	−0.0267	−0.0057	0.0210

Diff. = mean male FPC3 score − mean female FPC3 score.

In the full-sample analysis, the sex difference in Kinda FPC3 scores is intermediate between those of chacma and yellow baboons (Table 5). In the mean FPCA, which is less affected by sample composition, the Kinda shows the smallest male–female difference of any subspecies. This is consistent with the Kinda's lack of zygomatic breadth dimorphism illustrated in Figure 6.

5 | DISCUSSION

Cranial shape variation in *Papio* is largely driven by the interrelated factors of allometry and sexual dimorphism (Dunn et al., 2013; Freedman, 1962; Frost, 2013; Frost et al., 2003; Leigh, 2006), but prior studies have drawn varying conclusions as to the uniformity of these phenomena across subspecies (Frost et al., 2003; Leigh, 2006). Results of this study support a close relationship between size variation and sexual dimorphism in *Papio* but also reveal differences among subspecies in patterns of craniodental dimorphism.

5.1 | Dimorphism magnitude

The Kinda exhibits significantly lower values than other baboons for standard metrics of size and shape dimorphism (Table 2). However, when size dimorphism is accounted for, the Kinda's levels of cranial shape and canine dimorphism are unexceptional. Rather, it is the olive baboon whose dimorphism, especially in canine height, seems relatively low. In contrast with the chacma baboon, whose pronounced canine dimorphism reflects increased male size (Plavcan, 1998), low dimorphism in the olive baboon appears linked to an increase in female canine height relative to more "typical" subspecies (Figure 5a,b). Most baboon societies are characterized by high levels of interfemale competition (Swedell, 2011), which is generally associated with increased relative female canine height in anthropoids (Plavcan, 1998). However, Plavcan (1998) also found that anthropoid species with *coalitionary* female competition have relatively *smaller* female canines. The finding of relatively large female canines in the olive baboon, a coalitionary subspecies, is therefore counter to expectations based on the competition theory of female canine size variation (Plavcan, 1998). It is consistent, however, with the relatively low cranial form dimorphism also found in this subspecies, making it difficult to dismiss this result as an artifact of canine wear or small sample size. As our understanding of the diversity of baboon social systems increases, closer examination of female canine variation in *Papio* seems warranted (Fischer et al., 2017; Galat-Luong, Galat, & Hagell, 2006; Jolly et al., 2011; Phillips-Conroy et al., 2009a,b; Weyher et al., 2014).

5.2 | Dimorphism patterning

MANOVA of overall sexual dimorphism rejects the null hypothesis that shape dimorphism patterns are shared across *Papio* subspecies. However, statistically significant dimorphism vector angles were found only for the Kinda baboon versus the Guinea and hamadryas baboons, respectively. Dimorphism angle magnitudes do not show clear geographic or phylogenetic trends but are strongly correlated with both regression-vector and FPC1 angle matrices. This indicates that subspecies scaling differences, reflected in FPC1 angles and MANCOVA results, contribute substantially to sexual dimorphism variation. The Kinda baboon, with its consistently divergent dimorphism and scaling vectors, does appear to differ from other subspecies in its pattern of size-related dimorphism.

Vectors of size-independent sexual dimorphism (Figures 8b and 9b) summarize differences between males and females in midfacial breadth and anterior palate dimensions, the latter most likely reflecting canine size dimorphism (Frost et al., 2003; Singleton, 2002; Weston et al., 2004). Displacement of the Kinda on FPC3 (Figure 9b) reflects its greater relative facial breadth and other palate shape differences (Leigh, 2006). Effectively, male and, especially, female Kinda baboons appear slightly "masculinized" for their size relative to other subspecies. This finding is inconsistent with Leigh's (2006) hypothesis of relaxed male sexual selection, opening the door to other evolutionary scenarios. It may be simple coincidence that Kinda facial differences align with vectors of residual dimorphism. It is also possible that during Kinda evolution sexual dimorphism, as a source of standing variation, offered a path of least resistance similar to that provided by size (Marroig & Cheverud, 2005, 2009). Alternately, sexual selection favoring a relatively "masculine" phenotype in one sex, with correlated response in the other, might produce the displacement seen in Figures 8 and 9. Male sexual selection is most commonly invoked to explain papionin dimorphism patterns. However, the Kinda's unusual pattern of male–female affiliative behavior suggests that female sexual selection, operating in the context of female co-dominance, played a role in the evolution of Kinda sexual dimorphism (Clutton-Brock, 2007; Leigh, 2006; Weyher et al., 2014). Ongoing field studies of Kinda socioecology and biology should increase understanding of the historical influences that have shaped its cranial morphology and dimorphism patterns.

6 | CONCLUSIONS

This study investigated cranial size and shape dimorphism in *Papio* and tested the hypothesis that sexual dimorphism patterns in the diminutive Kinda baboon, *P. hamadryas kindae*, differ from those of other baboons. Consistent with prior studies (Dunn et al., 2013; Freedman, 1962; Frost, 2013; Frost et al., 2003; Leigh, 2006), we found a close relationship between size variation and sexual dimorphism in *Papio*, but also differences among subspecies in craniodental dimorphism patterns. The Kinda baboon exhibits significantly lower size and shape dimorphism than other baboons but its levels of cranial-shape dimorphism and canine dimorphism are unexceptional when size dimorphism is accounted for. The Kinda baboon differs from other subspecies in its patterns of allometry, size-related shape dimorphism, and residual (size-independent) shape dimorphism. Most notably, Kinda facial shape is slightly "masculinized" relative to size, especially in females, suggesting a possible role for female sexual selection in the evolution of Kinda dimorphism patterns. Further study of Kinda socioecology and biology is needed to understand the evolutionary history of the Kinda baboon's distinctive cranial form (Galat-Luong et al., 2006; Jolly et al., 2011; Phillips-Conroy et al., 2009a,b; Weyher et al., 2014).

ACKNOWLEDGMENTS

This research was supported by the Wenner-Gren Foundation (Grant 6436) and L.S.B. Leakey Foundation, S. Frost; NSF (BIR 902234), NYCEP; RF-CUNY (9-91980), E. Delson; the MWU Office of Research and Sponsored Programs; and the University of Oregon. Logistical support was provided by NYCEP, the Field Museum of Natural History, and the Department of Anthropology, University of Illinois–Urbana-Champaign. The authors thank the following institutions for access and curatorial assistance: American Museum of Natural History; Field Museum of Natural History; National Museum of Natural History–Smithsonian Institution; Powell-Cotton Museum; Royal Museum for Central Africa; University of California–Museum of Vertebrate Zoology; Natural History Museum, London; Museum National d'Histoire Naturelle; Forschungsinstitut Senkenberg; Ditsong Museum, Pretoria; and University of the Witwatersrand, Anatomy Department. For use of illustrations and photos, the authors thank K. Chiou; S.D. Nash, IUCN SSC Primate Specialist Group; and A. Weyher, Kasanka Baboon Project. For use of data and technical assistance, the authors thank S. Leigh, L. Pionek, and A. Martiny. They also thank Dr Peter Ellison, an anonymous Associate Editor, and two anonymous reviewers for constructive comments on the original version of the article. For ongoing contributions to this research, they thank E. Delson and the NYCEP Morphometrics Group. This article is NYCEP Morphometrics Contribution #106.

ORCID

Michelle Singleton http://orcid.org/0000-0003-0203-0185

REFERENCES

Bookstein, F. L. (1991). *Morphometric tools for landmark data: Geometry and biology*. Cambridge: Cambridge University Press.

Bookstein, F. L. (1996). Combining the tools of geometric morphometrics. In L. F. Marcus, M. Corti, A. Loy, G. J. P. Naylor, & D. E. Slice (Eds.), *Advances in morphometrics* (pp. 131–151). New York: Plenum Press.

Bowley, S. (2014). *mantel.SAS*. Retrieved April 12, 2017, from http://www.plant.uoguelph.ca/research/homepages/sbowley/assets/sas/mantel.sas

Burrell, A. S. (2009). *Phylogenetics and population genetics of central African baboons* (Ph.D. dissertation). New York University, New York.

Burrell, A. S., Jolly, C. J., Rogers, J., Phillips-Conroy, J., & Disotell, T. R. (2011). Inferring the dispersal behavior of the Kinda baboon (*Papio kindae*) from multilocus genetic data. *American Journal of Physical Anthropology*, *S51*, 99.

Burrell, A. S., Jolly, C. J., Tosi, A. J., & Disotell, T. R. (2009). Mitochondrial evidence for the hybrid origin of the kipunji, *Rungwecebus kipunji* (Primates: Papionini). *Molecular Phylogenetics and Evolution*, *51*, 340–348.

Chiou, K. L. (2013). A pilot description and categorization of Kinda baboon vocalizations. *American Journal of Physical Anthropology*, *S56*, 98.

Clutton-Brock, T. (2007). Sexual selection in males and females. *Science*, *318*, 1882–1885.

Delson, E., Terranova, C. J., Jungers, W. L., Sargis, E. J., Jablonski, N. G., & Dechow, P. C. (2000). Body mass in Cercopithecidae (Primates, Mammalia): Estimation and scaling in extinct and extant taxa. *Anthropological Papers of the American Museum of Natural History*, *83*, 1–159.

Drake, A. G., & Klingenberg, C. P. (2008). The pace of morphological change: Historical transformation of skull shape in St. Bernard dogs. *Proceedings of the Royal Society of London. B Biological Sciences*, *275*, 71–76.

Dryden, I. L., & Mardia, K. V. (1998). *Statistical shape analysis*. New York: John Wiley.

Dunn, J., Cardini, A., & Elton, S. (2013). Biogeographic variation in the baboon: Dissecting the cline. *Journal of Anatomy*, *223*, 337–352.

Fischer, J., Kopp, G. H., Dal Pasco, F., Goffe, A., Hammerschmidt, K., Kalbitzer, U., . . . Zinner, D. (2017). Charting the neglected West: The social system of Guinea baboons. *American Journal of Physical Anthropology*, *S63*, 15–31.

Fleagle, J. G. (2013). *Primate adaptation and evolution* (3rd ed.). New York: Academic Press.

Freedman, L. (1962). Growth of muzzle length relative to calvaria length in *Papio*. *Growth*, *26*, 117–128.

Freedman, L. (1963). A biometric study of *Papio cynocephalus* skulls from northern Rhodesia and Nyasaland. *Journal of Mammalogy*, *44*, 24–43.

Frost, S. R. (2013). Cranial shape variation in extant and fossil *Papio* and its implications for the evolution of the Kinda baboon. *American Journal of Physical Anthropology*, *S56*, 126.

Frost, S. R., Marcus, L. F., Reddy, D. P., Bookstein, F. L., & Delson, E. (2003). Cranial allometry, phylogeography and systematics of large-bodied papionins (Primates: Cercopithecinae) inferred from geometric morphometric analysis of landmark data. *Anatomical Record*, *275A*, 1048–1072.

Galat-Luong, A., Galat, G., & Hagell, S. (2006). The social and ecological flexibility of Guinea baboons: Implications for Guinea baboon social organization and male strategies. In *Reproduction and fitness in baboons: Behavioral, ecological, and life history perspectives* (pp. 105–121). New York: Springer.

Good, P. I. (2000). *Permutation tests: A practical guide to resampling methods for testing hypotheses*. New York: Springer.

Gower, J. C. (1966). Some distance properties of latent root and vector methods used in multivariate analysis. *Biometrika*, *53*, 325–338.

Greenfield, L. O., & Washburn, S. L. (1991). Polymorphic aspects of male anthropoid canines. *American Journal of Physical Anthropology*, *84*, 17–34.

Groves, C. (2001). *Primate taxonomy*. Washington, DC: Smithsonian Institution Press.

Grubb, P. (1999). Evolutionary processes implicit in distribution patterns of modern African mammals. In T. G. Bromage & F. Schrenk (Eds.), *African biogeography, climate change and human evolution* (pp. 150–164). New York: Oxford University Press.

Grubb, P., Butynski, T. M., Oates, J. F., Bearder, S. K., Disotell, T. R., Groves, C. P., & Struhsaker, T. T. (2003). Assessment of the diversity of African primates. *International Journal of Primatology*, *24*, 1301–1357.

Jolly, C. J. (1993). Species, subspecies, and baboon systematics. In W. H. Kimbel & L. B. Martin (Eds.), *Species, species concepts and primate evolution* (pp. 67–107). New York: Plenum.

Jolly, C. J. (2003). Cranial anatomy and baboon diversity. *Anatomical Record*, *275A*, 1043–1047.

Jolly, C. J., Burrell, A. S., Phillips-Conroy, J. E., Bergey, C. M., & Rogers, J. (2011). Kinda baboons (*Papio kindae*) and grayfoot chacma baboons (*P. ursinus griseipes*) hybridize in the Kafue River Valley, Zambia. *American Journal of Primatology*, *73*, 291–303.

Kingdon, J. (1997). *The Kingdon field guide to African mammals*. San Diego: Academic Press.

Klingenberg, C. P. (1996). Multivariate allometry. In L. F. Marcus, M. Corti, A. Loy, G. J. P. Naylor, & D. E. Slice (Eds.), *Advances in morphometrics* (pp. 23–49). New York: Plenum.

Klingenberg, C. P. (2016). Size, shape, and form: Concepts of allometry in geometric morphometrics. *Development Genes and Evolution*, *226*, 113–137.

Leigh, S. R. (2006). Cranial ontogeny of *Papio* baboons (*Papio hamadryas*). *American Journal of Physical Anthropology*, *130*, 71–84.

Leigh, S. R., & Cheverud, J. M. (1991). Sexual dimorphism in the baboon facial skeleton. *American Journal of Physical Anthropology*, *84*, 193–208.

Liedigk, R., Roos, C., Brameier, M., & Zinner, D. (2014). Mitogenomics of the Old World monkey tribe Papionini. *BMC Evolutionary Biology*, *14*, 176–187.

Marroig, G., & Cheverud, J. M. (2005). Size as a line of least evolutionary resistance: Diet and adaptive morphological radiation in New World monkeys. *Evolution*, *59*, 1128–1142.

Marroig, G., & Cheverud, J. M. (2009). Size as a line of least resistance II: Direct selection on size or correlated response due to constraints? *Evolution*, *64*, 1470–1488.

McNulty, K. P., Frost, S. R., & Strait, D. S. (2006). Examining affinities of the Taung child by developmental simulation. *Journal of Human Evolution*, *51*, 274–296.

Mitteroecker, P., & Gunz, P. (2009). Advances in geometric morphometrics. *Evolutionary Biology*, *36*, 225–247.

Mitteroecker, P., Gunz, P., Bernhard, M., Schaefer, K., & Bookstein, F. L. (2004). Comparison of cranial ontogenetic trajectories among great apes and humans. *Journal of Human Evolution*, *46*, 679–698.

Newman, T. K., Jolly, C. J., & Rogers, J. A. (2004). Mitochondrial phylogeny and systematics of baboons (*Papio*). *American Journal of Physical Anthropology*, *124*, 1, 17–27.

NYCEP (2013). *PRIMO: Primate Morphometrics Online*. Retrieved July 1, 2013, from http://primo.nycep.org/

O'Higgins, P., & Collard, M. (2002). Sexual dimorphism and facial growth in papionin monkeys. *Journal of Zoology London*, *257*, 255–272.

Phillips-Conroy, J. E., & Jolly, C. J. (1986). Changes in the structure of the baboon hybrid zone in the Awash National Park, Ethiopia. *American Journal of Physical Anthropology*, *71*, 337–350.

Phillips-Conroy, J. E., Jolly, C. J., Burrell, A. S., Rogers, J., & Weyher, A. H. (2009a). Genetic and behavioral observations of 'Kinda' baboons (*Papio cynocephalus kindae*) in Zambia. *American Journal of Physical Anthropology*, *S48*, 211.

Phillips-Conroy, J. E., Jolly, C. J., & Weyher, A. H. (2009b). Observations of 'Kinda' baboons (*Papio cynocephalus kindae*) in Zambia: Adult males as the active partner in male-female grooming dyads. *American Journal of Primatology*, *71*, 65.

Phillips-Conroy, J. E., Jolly, C. J., & Brett, F. L. (1991). Characteristics of hamadryas-like male baboons living in anubis baboon troops in the Awash hybrid zone, Ethiopia. *American Journal of Physical Anthropology*, *86*, 353–368.

Piepho, H. P. (2005). Permutation tests for the correlation among genetic distances and measures of heterosis. *Theoretical and Applied Genetics*, *111*, 95–99.

Plavcan, J. M. (1990). *Sexual dimorphism in the dentition of extant anthropoid primates* (Ph.D. dissertation). Duke University, Durham, NC.

Plavcan, J. M. (1993). Canine size and shape in male anthropoid primates. *American Journal of Physical Anthropology*, *92*, 201–216.

Plavcan, J. M. (1998). Correlated response, competition, and female canine size in primates. *American Journal of Physical Anthropology*, *107*, 401–416.

Plavcan, J. M., & Van Schaik, C. P. (1992). Intrasexual competition and canine dimorphism in anthropoid primates. *American Journal of Physical Anthropology*, *87*, 461–477.

Plavcan, J. M., Van Schaik, C. P., & Kappeler, P. M. (1995). Competition, coalitions and canine size in primates. *Journal of Human Evolution*, *28*, 245–276.

Samuels, A., & Altmann, J. (1986). Immigration of a *Papio anubis* male into a group of *Papio cynocephalus* baboons and evidence for an *anubis-cynocephalus* hybrid zone in Amboseli, Kenya. *International Journal of Primatology*, *7*, 131–138.

Šidák, Z. K. (1967). Rectangular confidence regions for the means of multivariate normal distributions. *Journal of the American Statistical Association*, *62*, 626–633.

Singleton, M. (2002). Patterns of cranial shape variation in the Papionini (Primates: Cercopithecinae). *Journal of Human Evolution*, *42*, 547–578.

Slice, D. E. (1998). *Morpheus et al.: Software for Morphometric Research*. Stony Brook University, Stony Brook, NY.

Slice, D. E. (2005). Modern morphometrics. In D. E. Slice (Ed.), *Modern morphometrics in physical anthropology* (pp. 1–45). New York: Kluwer Academic/Plenum Publishers.

Slice, D. E., Bookstein, F. L., Marcus, L. F., & Rohlf, F. J. (1996). Appendix I–A glossary for geometric morphometrics. In L. F. Marcus, M. Corti, A. Loy, G. J. P. Naylor, & D. E. Slice (Eds.), *Advances in morphometrics* (pp. 531–551). New York: Plenum Press.

Smith, R. J. (1981). Interspecific scaling of maxillary canine size and shape in female primates: Relationships to social structure and diet. *Journal of Human Evolution*, *10*, 165–173.

Swedell, L. (2011). African papionins: Diversity of social organization and ecological flexibility. In C. Campbell, A. Fuentes, K. C. MacKinnon, S. Bearder, & R. M. Stumpf (Eds.), *Primates in perspective* (2nd ed., pp. 241–277). New York: Oxford University Press.

Wall, J. D., Schlebusch, S. A., Alberts, S. C., Cox, L. A., Snyder-Mackler, N., . . . Tung, J. (2016). Genome-wide ancestry and divergence patterns from low-coverage sequencing data reveal a complex history of admixture in wild baboons. *Molecular Ecology*, *25*, 3469–3483.

Weston, E. M., Friday, A. E., Johnstone, R. A., & Schrenk, F. (2004). Wide faces or large canines? The attractive versus the aggressive primate. *Proceedings of the Royal Society of London B*, *271*, S416–S419.

Weyher, A. H., Phillips-Conroy, J. E., Fourrier, M. S., & Jolly, C. J. (2014). Male-driven grooming bouts in mixed-sex dyads of Kinda baboons (*Papio kindae*). *Folia Primatologica*, *85*, 178–191.

Wildman, D. E., Bergman, T. J., Al-Aghbari, A., Sterner, K. N., Newman, T. K., Phillips-Conroy, J. E., . . . Disotell, T. R. (2004). Mitochondrial evidence for the origin of hamadryas baboons. *Molecular Phylogenetics and Evolution*, *32*, 287–296.

Zelditch, M. L., Swiderski, D. L., Sheets, H. D., & Fink, W. L. (2004). *Geometric morphometrics for biologists: A primer*. New York: Elsevier Academic Press.

Zinner, D. (2013). Kinda baboon. In R. A. Mittermeier, A. B. Rylands, & D. E. Wilson (Eds.), *Handbook of the mammals of the world. Vol. 3: Primates* (pp. 661–662). Barcelona: Lynx Edicions.

Zinner, D., Groeneveld, L., Keller, C., & Roos, C. (2009). Mitochondrial phylogeography of baboons (*Papio* spp.)–indication for introgressive hybridization? *BMC Evolutionary Biology*, *9*, 83.

Zinner, D., Wertheimer, J., Liedigk, R., Groeneveld, L. F., & Roos, C. (2013). Baboon phylogeny as inferred from complete mitochondrial genomes. *American Journal of Physical Anthropology*, *150*, 133–140.

How to cite this article: Singleton M, Seitelman BC, Krecioch JR, Frost SR. Cranial sexual dimorphism in the Kinda baboon (*Papio hamadryas kindae*). *Am J Phys Anthropol*. 2017;164:665-678. https://doi.org/10.1002/ajpa.23304

APPENDIX 1: THREE-DIMENSIONAL CRANIOMETRIC LANDMARK DEFINITIONS (FROST ET AL., 2003)

Landmark	Dorsal/ventral	Definition
Midline		
Inion	D	Most posterior point on the occipital bone on midline
Bregma	D	Midline intersection of sagittal and coronal sutures
Glabella	D	Most anterior point on midline superior to nasofrontal suture
Nasion	D	Intersection of nasofrontal suture and midline
Rhinion	D	Most anterior point on fused nasal bones on midline
Nasospinale	D	Intersection of anterior nasal sill and midline
Prosthion	D	Most inferior point on septum between central incisors
Opisthion	V	Intersection of posterior foramen magnum margin and midline
Basion	V	Intersection of anterior foramen magnum margin and midline
Staphylion	V	Midline point on line tangent to the posterior palatine notch
Bilateral (R/L)		
Zygomaxillare inferior	D	Most inferior point on zygomaxillary suture
Zygomaxillare superior	D	Most superior point on zygomaxillary suture at orbital margin
Dacryon	D	Point of contact of lacrimal, maxillary, and frontal bones
Midtorus inferior	D	Approximate midpoint of superior orbital margin
Midtorus superior	D	Most anterior point on supraorbital torus directly superior to midtorus inferior
Frontomalare orbitale	D	Medial frontozygomatic suture at intersection with lateral orbital margin
Frontomalare temporale	D	Lateral frontozygomatic suture at intersection with temporal line
Porion	D	Most superior point on margin of external auditory meatus
Zygotemporale superior	D	Most superior point on the zygotemporal suture
Zygotemporale inferior	V	Most inferior point on the zygotemporal suture
Distal M3	V	Buccal alveolar process at level of distal M3
Mesial P3	V	Buccal alveolar process at level of canine-P3 alveolar septum

Because procrustes-based analyses do not accommodate specimens with missing landmarks, the 45-landmark set of Frost et al. (2003) was reduced to 34 landmarks to allow inclusion of more individuals.